Geophysical Research Letters

RESEARCH LETTER
10.1029/2019GL083837

Ocean Heat Transport Into the Barents Sea: Distinct Controls on the Upward Trend and Interannual Variability

Qiang Wang[1,2], Xuezhu Wang[1,3], Claudia Wekerle[1], Sergey Danilov[1,4], Thomas Jung[1,5], Nikolay Koldunov[1,6], Sigrid Lind[7,8], Dmitry Sein[1,9], Qi Shu[1,10], and Dmitry Sidorenko[1]

[1]Alfred-Wegener-Institut Helmholtz-Zentrum für Polar- und Meeresforschung (AWI), Bremerhaven, Germany, [2]Laboratory for Regional Oceanography and Numerical Modeling, Pilot National Laboratory for Marine Science and Technology (Qingdao), Qingdao, China, [3]College of Oceanography, Hohai University, Nanjing, China, [4]Department of Mathematics and Logistics, Jacobs University, Bremen, Germany, [5]Institute of Environmental Physics, University of Bremen, Bremen, Germany, [6]MARUM-Center for Marine Environmental Sciences, Bremen, Germany, [7]Institute of Marine Research, Tromsø, Norway, [8]Norwegian Meteorological Institute, Tromsø, Norway, [9]Shirshov Institute of Oceanology, Russian Academy of Science, Moscow, Russia, [10]First Institute of Oceanography, Ministry of Natural Resources, Qingdao, China

Key Points:
- Forcing responsible for the trend and interannual variability of ocean heat transported into the Barents Sea is disentangled
- The upward trend of the heat inflow stems from warming in the subpolar North Atlantic, while local wind accounts for half of its variance
- The location of the Atlantic Water boundary current relative to the Barents Sea entrance is crucial in determining the heat inflow

Supporting Information:
- Supporting Information S1

Correspondence to:
Q. Wang
Qiang.Wang@awi.de

Citation:
Wang, Q., Wang, X., Wekerle, C., Danilov, S., Jung, T., Koldunov, N., et al. (2019). Ocean heat transport into the Barents Sea: Distinct controls on the upward trend and interannual variability. *Geophysical Research Letters*, *46*, 13,180–13,190. https://doi.org/10.1029/2019GL083837

Received 23 MAY 2019
Accepted 2 SEP 2019
Accepted article online 6 SEP 2019
Published online 20 NOV 2019

Abstract Ocean heat transport through the Barents Sea Opening (BSO) has strong impacts on the Barents Sea ice extent and the climate. In this paper we quantified the contributions from different atmospheric forcing components to the trend and interannual variability of the BSO heat transport. Ocean-ice model simulations were conducted in which the interannual variation of atmospheric forcing was maintained only in or outside the Arctic in two different simulations. The sum of their BSO heat transport anomalies reasonably replicated the trend and variability from a hindcast simulation. The upward trend of the BSO heat transport mainly stems from the increasing ocean temperature in the subpolar North Atlantic. For the interannual variability, the local wind and upstream forcing are similarly important. The location of the Atlantic Water boundary current in the Nordic Seas, influenced by the cyclonic atmospheric circulation, is crucial in determining part of the BSO inflow variability.

1. Introduction

Ocean heat transported from the midlatitudes to the Arctic Ocean can impact Arctic sea ice coverage (Onarheim et al., 2014; Polyakov et al., 2010; Sandø et al., 2014) and contribute to Arctic amplification (Nummelin et al., 2017). In the Atlantic sector, Atlantic Water propagates northward through the Norwegian Sea and part of it enters the Barents Sea through the Barents Sea Opening (BSO; see Figure 1 a; Furevik, 2001; Ingvaldsen et al., 2002; Skagseth et al., 2008). Most of the ocean heat in the Barents Sea is released to the atmosphere, so this site plays an important role in the Arctic heat budget and climate variability (Årthun & Eldevik, 2016; Smedsrud et al., 2013). BSO heat transport drives the variability and declining trend of Barents Sea ice extent (Årthun et al., 2012), although sea ice advection also has an important impact (Lind et al., 2018). The decline of the Arctic winter sea ice extent is most profound in the Barents Sea (Cavalieri & Parkinson, 2012; Onarheim & Årthun, 2017), which could have strong implications for the weather and climate at lower latitudes (Cohen et al., 2014).

The increasing trend of Atlantic heat transport to the Nordic Seas in the past decades was influenced by changes in the strength and composition of the Atlantic Current in the northeast North Atlantic (Hakkinen & Rhines, 2009). The temperature anomalies in the North Atlantic can propagate persistently toward the Arctic Ocean through the Nordic Seas (Årthun et al., 2017). The variability of Atlantic Water inflow to the Nordic Seas is strongly influenced by wind forcing (Herbaut et al., 2017; Mork & Blindheim, 2000; Orvik & Skagseth, 2003; Skagseth, 2004; Skagseth & Orvik, 2002). Wind variability associated with the North Atlantic Oscillation (NAO) determines a large part of the inflow variability involving Ekman transport and barotropic adjustment (Nilsen et al., 2003; Sandø et al., 2012). Changes in steric sea surface height (SSH) could also contribute to the variability of Atlantic Water inflow (Hansen et al., 2010; Richter et al., 2012). Along-slope winds at the Norwegian coast can induce Ekman transport toward the coast and

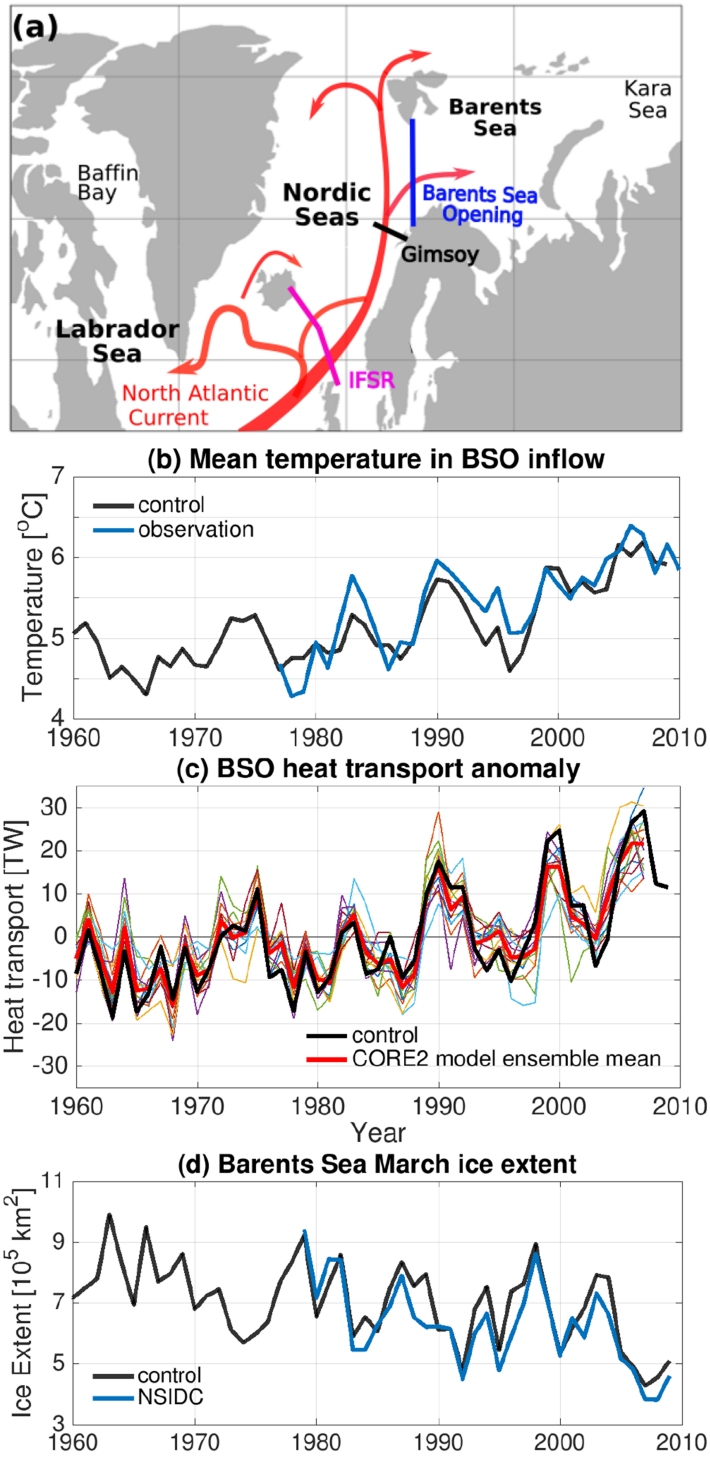

Figure 1. (a) Schematic of Atlantic Water circulation. (b) Annual mean temperature at Barents Sea Opening (BSO) in the control run and observation (Ingvaldsen et al., 2004). (c) Anomaly of ocean heat transport through the BSO in the control run (black thick line) and results from 14 CORE2 models (thin lines) described in Wang et al. (2016b). The ensemble mean of the CORE2 models is shown by the red thick line. (d) March Barents Sea ice extent in the control run and satellite observation (Fetterer et al., 2016). IFSR = Iceland-Faroe-Scotland-Ridge; CORE2 = Coordinated Ocean-ice Reference Experiments Phase II; NSIDC = National Snow and Ice Data Center.

generate an along-slope current, which explains the observed coherent variability of northward Atlantic Water transport in the Norwegian Sea (Skagseth, 2004). The eastward/westward extent of the Atlantic Water current in the Norwegian Sea, which is modulated by winds associated with the NAO variability, can influence the strength of the BSO inflow (Blindheim et al., 2000; Furevik, 1998; Zhang et al., 1998). Wind locally in the Barents Sea region can also influence the BSO volume transport through Ekman transport and setting up SSH gradient (Ingvaldsen et al., 2002, 2004).

Although possible mechanisms driving the variation of BSO volume and heat transport have been proposed, quantifying the relative contributions of different atmospheric forcing processes was not pursued yet. The recent increasing trend of ocean heat transport to the Arctic was found to be unprecedented in the past 2000 years based on sediment observations (Spielhagen et al., 2011), which cannot be explained only by internal variability or natural forcing (Jungclaus et al., 2014). Improved understanding of processes driving the variability and trend of BSO heat transport is required.

In this paper we propose a simple method to distinguish contributions to the variability and trend of BSO heat transport from atmospheric forcing in different geographical regions in ocean-ice model simulations. The interannual variation of atmospheric forcing is maintained only inside or outside the Arctic Ocean in two simulations. Summing their anomalies of BSO heat transport reasonably replicates that from a hindcast simulation. This makes it possible to quantify the relative roles of different atmospheric forcing components. Our focus is on variations on interannual and longer time scales.

In section 2 the model setups will be described. The model results are presented in section 3, followed by discussions and conclusions in sections 4 and 5, respectively.

2. Model Description

In this paper we use the Finite Element Sea Ice-Ocean Model (Wang et al., 2014), a multiresolution ocean general circulation model with both ocean and ice components based on an unstructured-mesh method (Danilov et al., 2015; Wang et al., 2008). Previous studies have shown that Finite Element Sea Ice-Ocean Model can reasonably simulate the ocean and sea ice in the Arctic Ocean and North Atlantic compared to observations and other models (e.g., Danabasoglu et al., 2016; Wang et al., 2016a, 2016b; Wang et al., 2016; Wang, Wekerle, Danilov, Wang, et al., 2018; Wang, Wekerle, Danilov, Koldunov, et al., 2018; Wekerle, Wang, Danilov, et al., 2017; Wekerle, Wang, von Appen, et al., 2017).

The employed setup is global with spatially varying horizontal resolution. The resolution in the North Atlantic is set to half of the first Rossby radius calculated from the ocean climatology, as done in Sein et al. (2017). In the Nordic Seas and Arctic Ocean the resolution is set to 9 km. In other parts of the global ocean the resolution is set to nominal 1° (mesh resolution is shown in the supporting information Figure S1). In the vertical, 47 z-levels are used with 10-m resolution in the upper 100 m.

The ocean is initialized with temperature and salinity climatology from Steele et al. (2001), and sea ice is initialized with a field obtained from a previous simulation. Two versions of the Coordinated Ocean-ice Reference Experiments Phase II (CORE2) atmospheric forcing data sets (Large & Yeager, 2009) are used. One version is the interannually varying forcing (IAVF) consisting of 6-hourly near-surface winds, air temperature and humidity, daily downward longwave and shortwave radiation, and monthly precipitation for the period 1948–2009. This forcing data set has been widely used in community efforts to assess ocean models and understand ocean dynamics (e.g., Danabasoglu et al., 2016), including studies on the Arctic Ocean (Ilicak et al., 2016; Wang et al., 2016b, 2016a). Therefore, using this forcing facilitates direct comparison with published multimodel results under the same forcing. The other CORE2 forcing version contains 1 year of forcing with the mean climatology of atmospheric fields and fluxes based on the period 1984–2000 (Large & Yeager, 2009). In this normal year forcing (NYF) the data temporal frequency is the same as in the IAVF. The air-sea turbulent fluxes are calculated following Large and Yeager (2009).

We conducted five simulations as described below:

1. control run: the hindcast simulation using the IAVF.
2. AO_vari: In the Arctic Ocean the IAVF is used, while outside the Arctic Ocean the NYF is used. The NYF is used repeatedly for every year. The domain of the Arctic Ocean is defined by the Arctic gateways near Fram Strait (76.5°N), BSO (17.5°E), Davis Strait (69°N), and Bering Strait (62°N).

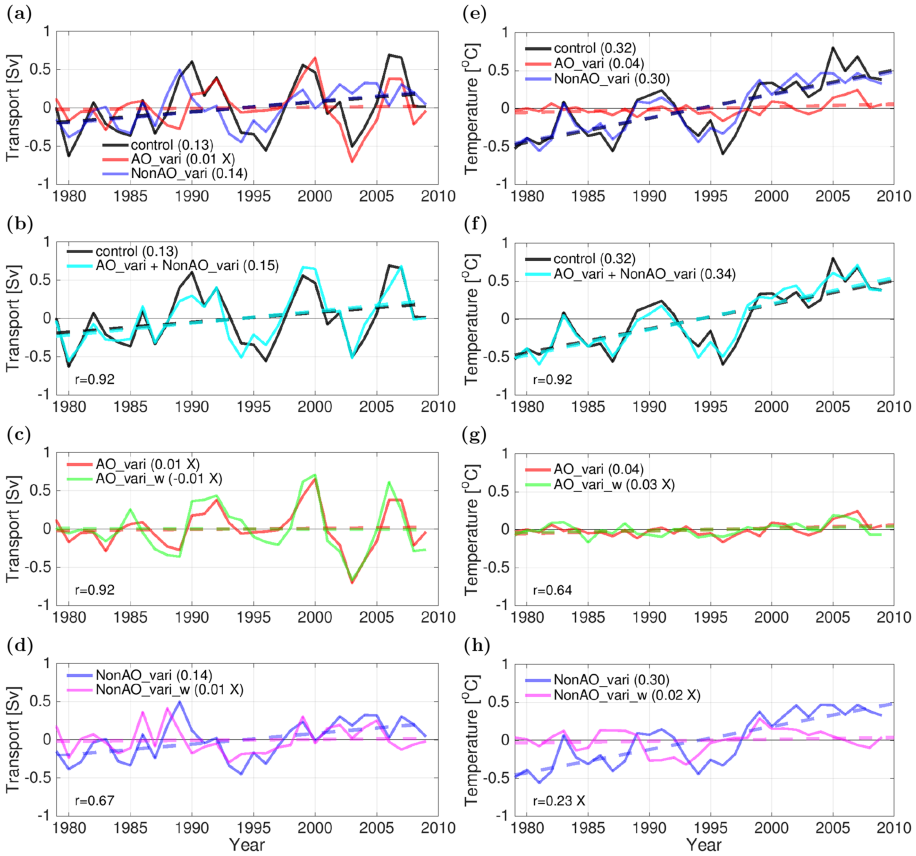

Figure 2. (a–d) Anomalies of annual mean warm water (>3 °C) volume transport through the Barents Sea Opening. (e–h) Anomalies of annual mean temperature within the warm water at the Barents Sea Opening. Dashed lines show corresponding linear trends. The values of linear trends (Sv/decade and °C/decade) are shown in the figure legends. The correlation coefficient between the detrended time series is also shown in (b)–(d) and (f)–(h). Linear trends and correlation coefficients not significant at the 95% level are indicated with an "X".

3. NonAO_vari: In the Arctic Ocean the NYF is used, while outside the Arctic Ocean the IAVF is used.
4. AO_vari_w: The same as the AO_vari run, but the atmospheric buoyancy forcing (the turbulent heat and freshwater fluxes computed from the bulk formulae and the downward radiation fluxes) in the Arctic Ocean is changed to the NYF. That is, only the wind (momentum) forcing inside the Arctic Ocean is taken from the IAVF.
5. NonAO_vari_w: The same as the NonAO_vari run, but the atmospheric buoyancy forcing outside the Arctic Ocean is changed to the NYF.

All the simulations were conducted from 1948 to 2009. For our purpose we focus on the results for the satellite period 1979–2009.

3. Results

In the satellite period the ocean inflow temperature at the BSO has a strong increasing trend (Ingvaldsen et al., 2004), which is well represented by the control simulation (Figure 1b). The simulated ocean heat transport through the BSO is 74 TW (referenced to 0 °C), very close to the observed value (70±5 TW using the same reference temperature; Smedsrud et al., 2013). Actually, the variability and increasing trend of the ocean heat transport in the control run are very similar to the ensemble mean of 14 CORE2 models described in Wang et al., 2016b (2016b; Figure 1c). Furthermore, the observed decline of winter sea ice extent in the Barents Sea in the satellite period is well reproduced in the simulation (Figure 1d).

3.1. Decomposing the Trend and Variability

Without the atmospheric forcing interannual variation outside the Arctic Ocean in the AO_vari run, the ocean volume transport and the mean temperature at the BSO do not have the significant upward trends

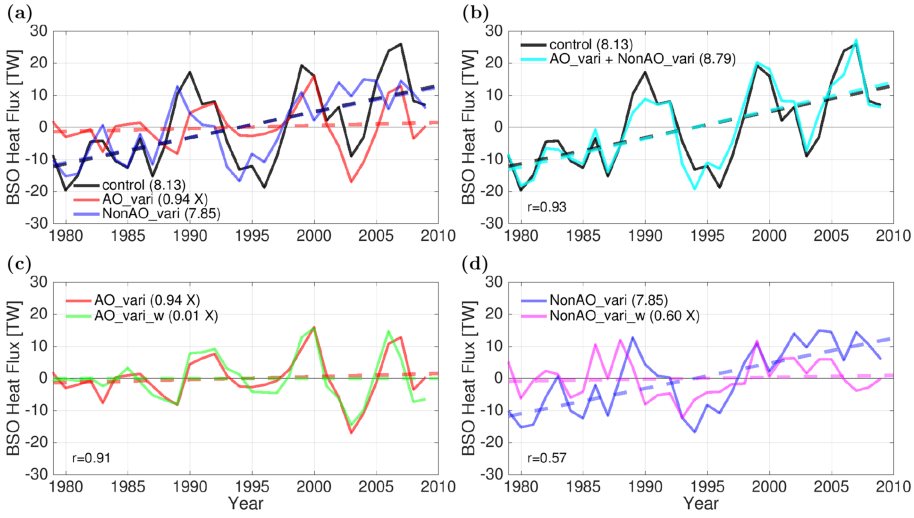

Figure 3. (a–d) Anomalies of ocean heat transport through the Barents Sea Opening (BSO). Dashed lines show corresponding linear trends. The values of linear trends (TW/decade) are shown in the figure legends. The correlation coefficient between the detrended time series is shown in (b)–(d). Linear trends and correlation not significant at the 95% level are indicated with an "X".

obtained in the control run (Figures 2a and 2e). The trends in the control run are mainly caused by the forcing outside the Arctic Ocean as shown by the NonAO_vari run. With forcing variability only in the Arctic Ocean, the ocean volume transport shows strong interannual variability (Figure 2a) but the temperature does not (Figure 2e). Summing the anomalies from the AO_vari and NonAO_vari runs well replicates the control run results for both the volume transport (Figure 2b) and temperature (Figure 2f). It is also obvious that winds in the Arctic Ocean are responsible for the volume transport variability in the AO_vari run (Figure 2c). On the contrary, the buoyancy forcing outside the Arctic Ocean is responsible not only for part of the interannual variability of the volume transport and temperature but also for all their upward trends in NonAO_vari (Figures 2d and 2h).

Accordingly, eliminating the interannual variation in the atmospheric forcing outside the Arctic Ocean removes most of the upward trend of the BSO heat transport (by about 90%), as shown by the AO_vari run (Figure 3a). About half of the variance of the detrended heat transport is retained in this run. When the interannual variation in the atmospheric forcing is eliminated in the Arctic Ocean in the NonAO_vari run, the model can reproduce nearly all the trend and about half of the variance. Summing the heat transport anomalies from the AO_vari and NonAO_vari runs well replicates that of the control run (Figure 3b), as expected from the results of volume transport and temperature (Figures 2b and 2f). The residual (uncertainty) of decomposing the forcing geographically is 8% for the linear trend and 15% for the variance of the BSO heat transport. The variability of BSO heat transport is mainly due to the variation of ocean velocity for the part that is driven by the local wind, while both the variations of ocean velocity and temperature contribute to the heat transport variability for the part originating from upstream (Figure S2).

The interannual variability of the BSO heat transport associated with the local Arctic atmospheric forcing can be mainly attributed to winds (Figure 3c). The upward trend of the BSO heat transport originating from upstream is predominantly due to the atmospheric buoyancy forcing—the only difference between the two model settings in Figure 3d. The heat transports are significantly correlated between the NonAO_vari and NonAO_vari_w runs (0.57, detrended), and the variance in NonAO_vari_w is about 60% of that in NonAO_vari. The correlation for the heat transport between these two runs is lower than that for the volume transport (0.67, Figure 2d), because the buoyancy forcing has a significant impact on the temperature variability (Figure 2h).

3.2. Responsible Processes

The upward trend of the Atlantic Water volume transport into the Nordic Seas through the Iceland-Faroe-Scotland-Ridge (IFSR) is not significant as shown by the observation and control simulation (Figure S3). Although the small upward trends of Atlantic Water volume transport are the same in

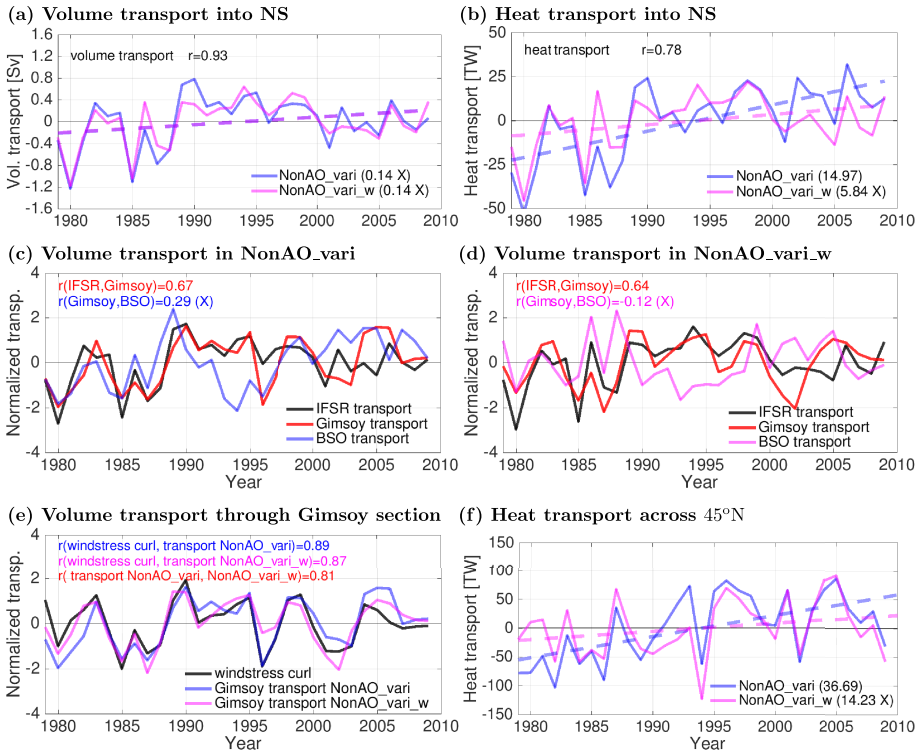

Figure 4. (a) The anomalies of warm water (>5 °C) volume transport through the Iceland-Faroe-Scotland Ridge (IFSR) in NonAO_vari and NonAO_vari_w runs. (b) The same as (a) but for ocean heat trasnport. (c) Normalized warm water volume transport at IFSR and Gimsoy sections (>5 °C) and at the Barents Sea Opening (BSO; >3 °C) in NonAO_vari. (d) The same as (c) but for NonAO_vari_w. (e) Normalized wind stress curl averaged in the Nordic Seas and the warm water (>5 °C) volume transport at the Gimsoy section. (f) Anomalies of ocean heat transport across 45°N in the upper 300 m in the North Atlantic; positive values mean stronger northward transport. In (a, b, f) the dashed lines show corresponding linear trends, and the values of the trends are shown in the figure legends (Sv/decade and TW/decade for volume and heat transports, respectively). The correlation coefficients between the curves are shown at the top of panels (a)–(e). Linear trends and correlation coefficients not significant at the 95% level are indicated with an "X." The locations of IFSR, Gimsoy, and BSO sections are indicated in Figure 1a.

NonAO_vari and NonAO_vari_w (Figure 4a), the trend of heat transport through the IFSR is more than twice higher in NonAO_vari (Figure 4b), implying that the inflow temperature in NonAO_vari has an upward trend. The ocean heat content (represented by vertically averaged temperature in the upper 300 m) in both the NonAO_vari and control runs clearly shows a warming trend in the subpolar North Atlantic (Figures 5a and 5b). In these two runs the ocean warming signal is also present in the Norwegian and Barents Seas. When the variation in the atmospheric buoyancy forcing is eliminated in NonAO_vari_w, the warming trend in the subpolar North Atlantic is largely absent (Figure 5c). Although there is a small upward trend in the IFSR heat transport associated with the insignificant trend of ocean volume transport in NonAO_vari_w (Figures 4a and 4b), the ocean warming signal is damped by surface heat loss in the Norwegian Sea so that the heat inflow trend at the BSO is negligible compared to the NonAO_vari run (Figure 3d).

Both the ocean volume and heat transports into the Nordic Seas are significantly correlated between the NonAO_vari and NonAO_vari_w runs (Figures 4a and 4b). In each run, the heat transport is also highly correlated with the ocean volume transport. These indicate that the wind forcing predominantly drives the interannual variability of volume and heat transport to the Nordic Seas. The regression of the sea level pressure (SLP) on the IFSR volume transport reveals an NAO-like pattern (Figure 5d). Our result is consistent with previous findings on the role of winds associated with the NAO variability in setting up SSH gradient and thus determining the Atlantic Water inflow to the Nordic Seas (e.g., Nilsen et al., 2003; Sandø et al., 2012).

The ocean volume transport of warm water (>5 °C) at the Gimsoy section, in a short distance upstream the BSO (location shown in Figure 1a), is still significantly correlated with the inflow through the IFSR in both the NonAO_vari and NonAO_vari_w runs (Figures 4c and 4d). It was found that the northward inflow along

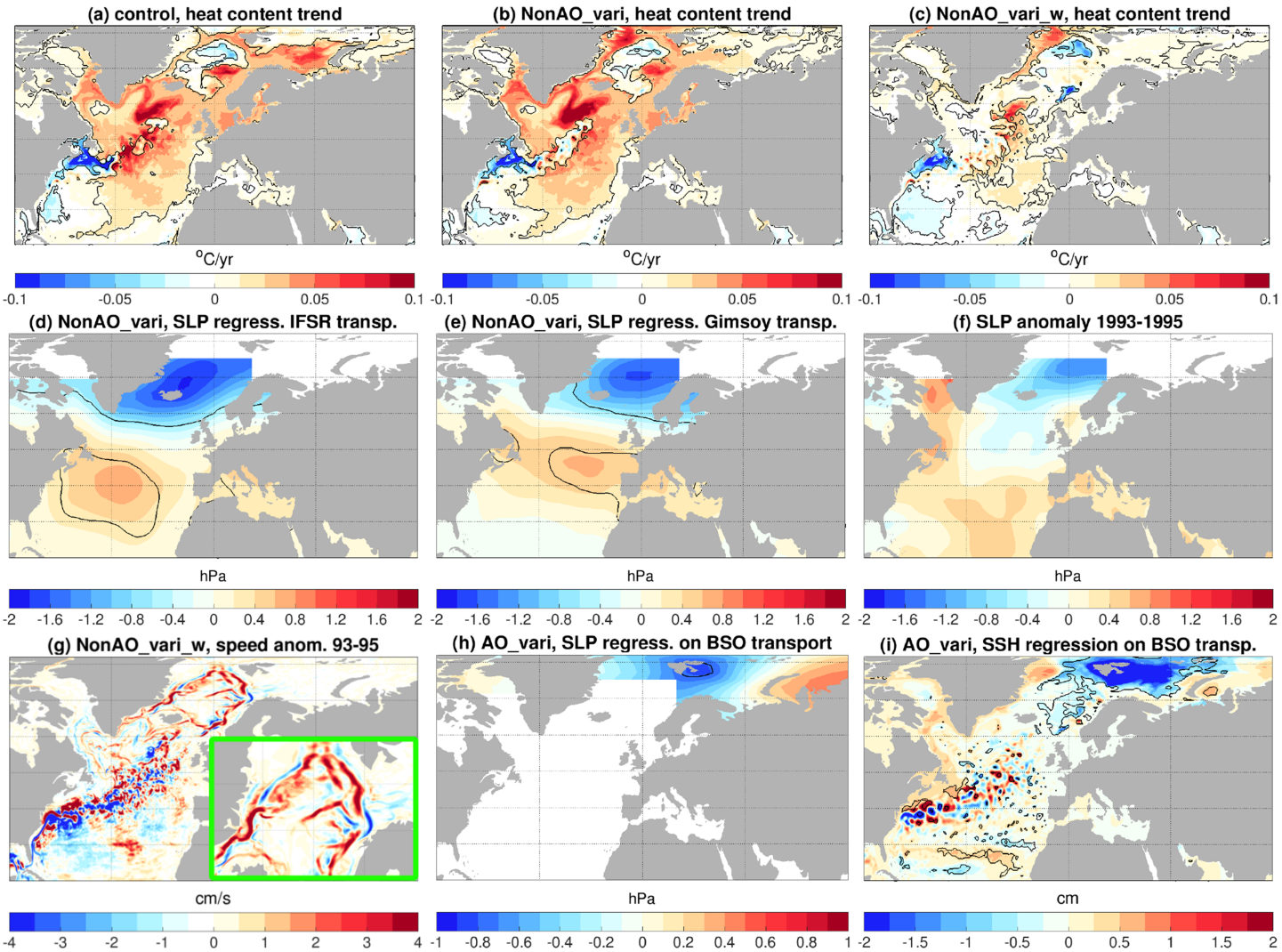

Figure 5. (a–c) Linear trends of heat content in the upper 300 m (°C/year) in (a) control, (b) NonAO_vari, and (c) NonAO_vari_w runs. (d, e) Regression coefficients between sea level pressure (SLP) and warm water volume transports through the Iceland-Faroe-Scotland Ridge (IFSR) and the Gimsoy section in hectopascal per standard deviation volume transport for NonAO_vari. (f) Anomaly of the composite SLP relative to the 1979–2009 mean for years (1993–1995) when Gimsoy transport is high, while the Barents Sea Opening (BSO) inflow is low. (g) The same as (f) but for the anomaly of the upper 200-m ocean speed in NonAO_vari_w. The Nordic Seas are enlarged and shown in the inset. (h) The regression of SLP on warm water volume transport through the BSO in hectopascal per standard deviation volume transport for AO_vari. (i) The same as (h) but for the regression of sea surface height (SSH). The black contours show the 95% confidence level for the trend and regression.

the Norwegian coast has coherent variability without time lags, which implies a large-scale barotropic forcing transfer with the fingerprint of the NAO variability (Skagseth, 2004; Skagseth et al., 2008). Indeed, the regression of SLP on the Gimsoy section warm water transport shows a NAO-like pattern (Figure 5e). The wind stress curl (or Ekman pumping) over the Nordic Seas drives the barotropic response of the cyclonic circulation (Isachsen et al., 2003). Therefore, it can explain the variability of the simulated Gimsoy section transports (Figure 4e). The transports are significantly correlated between the two runs (Figure 4e), which clearly indicates that the variability is largely wind driven.

However, despite the short distance from the Gimsoy section to the BSO, the warm water volume transport is not significantly correlated between the two sections for both the NonAO_vari and NonAO_vari_w runs (Figures 4c and 4d). The explanation is that the inflow to the Barents Sea through the BSO is determined not only by the strength of the current upstream but also by the location of the current relative to the continental shelf break. For example, in the period 1993–1995 when the Gimsoy section transport is in a high phase, the SLP has a negative anomaly in the Nordic Seas (Figure 5f), which strengthens the cyclonic

circulation and Atlantic Water current in the Nordic Seas (Figure 5g). In the meantime, the onshore extension of the Atlantic Water current in front of the BSO is weakened (Figure 5g), which is found not only in NonAO_vari_w but also in NonAO_vari and the control runs (Figure S4). The overall result is a reduction in the BSO inflow in these years (Figures 4c and 4d).

When the IAVF is maintained only inside the Arctic Ocean in the AO_vari run, the regression of SLP on the BSO transport shows a pattern with low pressure around the Svalbard and high pressure centered at the southwestern Kara Sea (Figure 5h). The wind anomaly associated with this pattern can lower the SSH on the Svalbard side through Ekman divergence (Figure 5i), thus increasing the SSH gradient and the BSO transport, consistent to previous studies on the role of local wind forcing (Ingvaldsen et al., 2002, 2004; Lien et al., 2013, 2017; Muilwijk et al., 2018; Skagseth et al., 2011).

4. Discussions

4.1. Warming in the Subpolar North Atlantic

Our simulations show that the ocean heat entering the subpolar North Atlantic through its southern boundary at 45°N has a significant upward trend in NonAO_vari (Figure 4f). Increasing ocean temperature leads to this upward trend because there is no significant trend in the ocean volume transport at 45°N (not shown).

Despite the increase in ocean surface temperature in the NonAO_vari run (Figure 5b), the ocean heat loss to the atmosphere in the subpolar region does not increase significantly with time (Figure S5c). This is because of the increasing trend in the air temperature (cf. Figures S5a and S5b). That is, the atmospheric warming in the subpolar North Atlantic provides a condition that the additional ocean heat advected to this region from the south is not significantly lost to the atmosphere on the way. Therefore, the warming trend in the subpolar North Atlantic is maintained by both the enhanced ocean heat transport through its southern boundary and the local atmospheric warming.

4.2. Impact of Nordic Seas Circulation on BSO Heat Inflow

We showed that the location of the Atlantic Water current relative to the continental shelf break in front of the BSO is crucial in determining the BSO inflow strength. In the period 1993–1995, the BSO inflow is weak despite that the Gimsoy section transport is high (Figures 4c and 4d). There are also years when both the Gimsoy section and BSO transports are high (1999 and 2005; Figures 4c and 4d). In these years the Atlantic Water current along the continental slope is strengthened, while the onshore extension of the current toward the BSO is also stronger (Figure S6b). As expected, the SLP has a negative anomaly (Figure S7b) and the wind stress curl is in a positive phase (Figure 4e). In these years the negative SLP anomaly has a spatial pattern extending more to the Norwegian Sea compared to the 1993–1995 period (cf. Figures S7a and S7b), which helps to maintain the Atlantic Water current in close proximity to the shelf break of the BSO (Figure S6b). Two different cases when the Gimsoy section transport is low are also identified according to Figures 4c and 4d: the BSO transport could be in a low phase (1980 and 1984; Figure S6c) or in a high phase (1988, 2001, and 2002; Figure S6d). In both cases the SLP in the Nordic Seas has positive anomalies as expected (Figures S7c and S7d). The two phases are different in the relative location of the SLP anomalies. When the positive SLP anomaly is located at the center of the Nordic Seas (Figure S7d), the weakened gyre circulation allows the warm water boundary current to be closer to the BSO (Figure S6d). On the contrary, when the positive SLP anomaly is over the eastern Nordic Seas (Figure S7c), the center of the cyclonic atmospheric and ocean circulation, thus the Atlantic Water boundary current, tends to be farther from the BSO (Figure S6c).

The response of the BSO transport to the wind forcing for the few periods mentioned above is very similar between NonAO_vari and NonAO_vari_w. There are also years when the BSO transport has different tendency between these two runs. The correlation of volume transports between these two runs reduces from 0.81 at the Gimsoy section to 0.67 at the BSO. The reduction in the correlation is relatively small, implying that wind forcing over the Nordic Seas plays a crucial role in determining the BSO volume transport variability for the part of upstream origin.

4.3. Oceanic Linkage Between the North Atlantic and Barents Sea

The variation of Atlantic Water inflow to the Nordic Seas is highly correlated with the NAO-like wind forcing, which influences the ocean volume inflow through setting up SSH gradient (Bringedal et al., 2018;

Sandø et al., 2012). Skagseth (2004) found coherent (negligible phase lag) variations of the Atlantic Water current along the Norwegian coast toward the Barents Sea, which are forced by the NAO-like wind forcing and indicate barotropic transfer mechanisms. The correlation of ocean currents between the BSO and a transect at the southern end of the Norwegian Sea is only moderate (Skagseth et al., 2008), and one possible reason is that the eastward/westward extent of the Atlantic Water current in the Norwegian Sea can influence the strength of the BSO inflow (Blindheim et al., 2000; Furevik, 1998; Zhang et al., 1998). Local winds at the BSO can also significantly influence the strength of the inflow through changing the SSH gradient across the BSO (Ingvaldsen et al., 2002, 2004). Our model results are consistent with the processes summarized above, which control the variability of Atlantic Water transport along the pathway starting from the northern North Atlantic to the Barents Sea. We found that the location of the Atlantic Water boundary current relative to the shelf break of the BSO is crucial in determining the strength of the BSO inflow. It turned out to be even more important than the strength of the Atlantic Water current upstream the BSO in some years. We also quantified that local winds at the BSO alone are responsible for about half of the total variance of the BSO inflow.

We found that the warming trend of the subpolar North Atlantic supplies the increase of heat transport through the BSO, consistent with the persistent propagation of temperature anomalies from the North Atlantic to the Nordic Seas identified by Årthun et al. (2017). The linkage between the upper ocean temperature in the North Atlantic and the BSO heat transport implies certain predictability of the ocean heat transport to the Barents Sea and sea ice conditions therein, in support of previous studies on Arctic predictability (Årthun et al., 2017; Yeager et al., 2015). We note that the interannual variability of BSO heat transport induced by local winds is so strong that it could mask the variability from upstream, which makes it challenging to predict the Barents Sea environment over short periods by just using North Atlantic information.

In our studied period, local winds at the BSO have no significant trend and thus the increasing trend of BSO volume and heat transports originates from upstream forcing. However, possible changes in local winds in future warming climate could also cause trends in BSO ocean volume transport (Årthun et al., 2019).

5. Conclusions

In this paper we quantified the contributions of different atmospheric forcing components to the trend and variability of BSO volume and heat transports for the period 1979–2009. The interannual variation of the atmospheric forcing is maintained only in or outside the Arctic Ocean in two different simulations. The sum of the BSO transport anomalies from these two simulations can replicate the linear trend and interannual variability from the hindcast simulation, implying that the system is largely linear in terms of the forcing processes that we focus on. In addition, we carried out sensitivity experiments to distinguish the relative importance of buoyancy and wind forcing.

We found that nearly all the upward trend of the BSO heat transport in the studied period originates from the atmospheric buoyancy forcing over the North Atlantic and Nordic Seas. The ocean warming trend in the northern North Atlantic, caused by both enhanced ocean heat transport from lower latitudes and local atmospheric warming, feeds the significant upward trend in the heat transport into the Nordic Seas and thus into the Barents Sea.

Although wind forcing locally in the Barents Sea region has very minor contribution to the upward trend of the BSO heat transport, it accounts for about half of the variance through influencing the ocean volume transport by changing the SSH gradient across the BSO. Wind and buoyancy forcing together from upstream contributes to about half of the BSO heat transport variance through influencing both the volume transport and temperature.

The wind variability over the Nordic Seas resembling the NAO largely determines the variability of the gyre circulation in the Nordic Seas and thus the coherent variability of the Atlantic Water current along the Norwegian slope, but the details in the SLP pattern and winds play a crucial role in driving the variability of BSO transport. That is, not only the strength of the Atlantic Water current but also the proximity of the boundary current to the BSO are important. We identified events in which the Atlantic Water boundary current in the Norwegian Sea is strong (weak) , while the BSO inflow is weak (strong). These events can be

masked in the presence of local wind variability at the BSO, when the latter can cause stronger variability in the BSO inflow. Our decomposition of the forcing helped to reveal these events.

Our simulations did not cover the recent years when a few interesting climate events have happened; for example, the subpolar North Atlantic changed to a cooling phase for some years (Josey et al., 2018) and the Norwegian Sea experienced a decoupling of the temperature and salinity (Mork et al., 2019). We expect that the numerical method used in this study can be extended to understand these changes.

Acknowledgments
This work is supported by the German Helmholtz Climate Initiative REKLIM (Regional Climate Change, Q. Wang and D. Sidorenko), by the projects S1 (Diagnosis and Metrics in Climate Models) and S2 (improved parameterizations and numerics in climate models) of the Collaborative Research Centre TRR 181 "Energy Transfer in Atmosphere and Ocean" funded by the Deutsche Forschungsgemeinschaft (DFG, German Research Foundation) with Projektnummer 274762653 (N. Koldunov, S. Danilov, and T. Jung), the EC project PRIMAVERA under Grant Agreement 641727 (D. Sein and T. Jung), and the state assignment of FASO Russia (theme No. 0149-2019-0015, D. Sein). The observational data of sea ice and ocean temperature used in this paper were obtained online (https://nsidc.org/data/seaice_index/ and https://ocean.ices.dk/iroc/). The model data are available online (https://swiftbrowser.dkrz.de/public/dkrz_035d8f6ff058403bb42f8302e6-badfbc/Wang_2019/) or by contacting the corresponding author.

References

Årthun, M., & Eldevik, T. (2016). On anomalous ocean heat transport toward the Arctic and associated climate predictability. *Journal of Climate*, *29*, 689–704.

Årthun, M., Eldevik, T., & Smedsrud, L. H. (2019). The role of Atlantic heat transport in future Arctic winter sea ice loss. *Journal of Climate*, *32*, 3327–3341.

Årthun, M., Eldevik, T., Smedsrud, L. H., Skagseth, O., & Ingvaldsen, R. B. (2012). Quantifying the influence of Atlantic heat on Barents Sea ice variability and retreat. *Journal of Climate*, *25*, 4736–4743.

Årthun, M., Eldevik, T., Viste, E., Drange, H., Furevik, T., Johnson, H. L., & Keenlyside, N. S. (2017). Skillful prediction of northern climate provided by the ocean. *Nature Communications*, *8*, 15875.

Blindheim, J., Borovkov, V., Hansen, B., Malmberg, S., Turrell, W., & Osterhus, S. (2000). Upper layer cooling and freshening in the Norwegian Sea in relation to atmospheric forcing. *Deep Sea Research Part I: Oceanographic Research Papers*, *47*, 655–680.

Bringedal, C., Eldevik, T., Skagseth, O., Spall, M., & Osterhus, S. (2018). Structure and forcing of observed exchanges across the Greenland Scotland Ridge. *Journal of Climate*, *31*, 9881–9901.

Cavalieri, D. J., & Parkinson, C. L. (2012). Arctic sea ice variability and trends, 1979–2010. *Cryosphere*, *6*, 881–889.

Cohen, J., Screen, J. A., Furtado, J. C., Barlow, M., Whittleston, D., Coumou, D., et al. (2014). Recent Arctic amplification and extreme mid-latitude weather. *Nature Geoscience*, *7*, 627–637.

Danabasoglu, G., Yeager, S. G., Kim, W. M., Behrens, E., Bentsen, M., Bi, D., et al. (2016). North Atlantic simulations in Coordinated Ocean-ice Reference Experiments phase II (CORE-II). Part II: Inter-annual to decadal variability. *Ocean Modelling*, *97*, 65–90.

Danilov, S., Wang, Q., Timmermann, R., Iakovlev, N., Sidorenko, D., Kimmritz, M., et al. (2015). Finite-Element Sea Ice Model (FESIM), version 2. *Geoscientific Model Development*, *8*, 1747–1761.

Fetterer, F., Knowles, K., Meier, W., & Savoie, M. (2016). Sea ice index. Boulder, Colorado USA: National snow and ice data center. Digital media. updated daily.

Furevik, T. (1998). On the Atlantic Water flow in the Nordic Seas: Bifurcation and variability (Unpublished doctoral dissertation), University of Bergen, Bergen, Norway.

Furevik, T. (2001). Annual and interannual variability of Atlantic Water temperatures in the Norwegian and Barents Seas: 1980–1996. *Deep-sea Research I*, *48*, 383–404.

Hakkinen, S., & Rhines, P. B. (2009). Shifting surface currents in the northern North Atlantic Ocean. *Journal of Geophysical Research*, *114*, C04005. https://doi.org/10.1029/2008JC004883

Hansen, B., Hátún, H., Kristiansen, R., Olsen, S. M., & Osterhus, S. (2010). Stability and forcing of the Iceland-Faroe inflow of water, heat, and salt to the Arctic. *Ocean Science*, *6*, 1013–1026.

Herbaut, C., Houssais, M.-N., Close, S., & Blaizot, A.-C. (2017). On the spatial coherence of the Atlantic Water inflow across the Nordic Seas. *Journal of Geophysical Research: Oceans*, *122*, 4346–4363. https://doi.org/10.1002/2016JC012566

Ilicak, M., Drange, H., Wang, Q., Gerdes, R., Aksenov, Y., Bailey, D., et al. (2016). An assessment of the Arctic Ocean in a suite of inter-annual CORE-II simulations. Part III: Hydrography and fluxes. *Ocean Modelling*, *100*, 141–161.

Ingvaldsen, R., Asplin, L., & Loeng, H. (2004). Velocity field of the western entrance to the Barents Sea. *Journal of Geophysical Research*, *109*, C03021. https://doi.org/10.1029/2003JC001811

Ingvaldsen, R., Loeng, H., & Asplin, L. (2002). Variability in the Atlantic inflow to the Barents Sea based on a one-year time series from moored current meters. *Continental Shelf Research*, *22*, 505–519.

Isachsen, P. E., LaCasce, J. H., Mauritzen, C., & Häkkinen, S. (2003). Wind-driven variability of the large-scale recirculating flow in the Nordic Seas and Arctic Ocean. *Journal of Physical Oceanography*, *33*, 2534–2550.

Josey, S. A., Hirschi, J. J. M., Sinha, B., Duchez, A., Grist, J. P., & Marsh, R. (2018). The recent Atlantic cold anomaly: Causes, consequences, and related phenomena. *Annual Review of Marine Science*, *10*, 475–501.

Jungclaus, J., Lohmann, K., & Zanchettin, D. (2014). Enhanced 20th-century heat transfer to the Arctic simulated in the context of climate variations over the last millennium. *Climate of the Past*, *10*, 2201–2213.

Large, W. G., & Yeager, S. G. (2009). The global climatology of an interannually varying air-sea flux data set. *Climate Dynamics*, *33*, 341–364.

Lien, V. S., Schlichtholz, P., Skagseth, O., & Vikebø, F. B. (2017). Wind-driven Atlantic Water flow as a direct mode for reduced Barents Sea ice cover. *Journal Climate*, *30*, 803–812.

Lien, V. S., Vikebø, F. B., & Skagseth, O. (2013). One mechanism contributing to co-variability of the Atlantic inflow branches to the Arctic. *Nature Communications*, *4*, 1488.

Lind, S., Ingvaldsen, R. B., & Furevik, T. (2018). Arctic warming hotspot in the northern Barents Sea linked to declining sea-ice import. *Nature Climate Change*, *8*, 634–639.

Mork, K., & Blindheim, J. (2000). Variations in the Atlantic inflow to the Nordic Seas, 1955–1996. *Deep Sea Research Part I: Oceanographic Research Papers*, *47*, 1035–1057.

Mork, K., Skagseth, O., & Soiland, H. (2019). Recent warming and freshening of the Norwegian Sea observed by Argo data. *Journal of Climate*, *32*, 3695–3705.

Muilwijk, M., Smedsrud, L. H., Ilicak, M., & Drange, H. (2018). Atlantic water heat transport variability in the 20th century Arctic Ocean from a global ocean model and observations. *Journal of Geophysical Research: Oceans*, *123*, 8159–8179. https://doi.org/10.1029/2018JC014327

Nilsen, J. E. O., Gao, Y., Drange, H., Furevik, T., & Bentsen, M. (2003). Simulated North Atlantic-Nordic Seas water mass exchanges in an isopycnic coordinate OGCM. *Geophysical Research Letters*, *30*(10), 1536. https://doi.org/10.1029/2002GL016597

Nummelin, A., Li, C., & Hezel, P. (2017). Connecting ocean heat transport changes from the midlatitudes to the Arctic Ocean. *Geophysical Research Letters*, *44*, 1899–1908. https://doi.org/10.1002/2016GL071333

Onarheim, I. H., & Årthun, M. (2017). Toward an ice-free Barents Sea. *Geophysical Research Letters*, *44*, 8387–8395. https://doi.org/10.1002/2017GL074304

Onarheim, I. H., Smedsrud, L. H., Ingvaldsen, R. B., & Nilsen, F. (2014). Loss of sea ice during winter north of Svalbard. *Tellus A: Dynamic Meteorology and Oceanography*, *66*, 23933. https://doi.org/10.3402/tellusa.v66.23933

Orvik, K., & Skagseth, O. (2003). The impact of the wind stress curl in the North Atlantic on the Atlantic inflow to the Norwegian Sea toward the Arctic. *Geophysical Research Letters*, *30*(17), 1884. https://doi.org/10.1029/2003GL017932

Polyakov, I., Timokhov, L., Alexeev, V., Bacon, S., Dmitrenko, I., Fortier, L., et al. (2010). Arctic ocean warming contributes to reduced polar ice cap. *Journal of Physical Oceanography*, *40*(12), 2743–2756.

Richter, K., Segtnan, O. H., & Furevik, T. (2012). Variability of the Atlantic inflow to the Nordic Seas and its causes inferred from observations of sea surface height. *Journal of Geophysical Research*, *117*, C04004. https://doi.org/10.1029/2011JC007719

Sandø, A., Gao, Y., & Langehaug, H. R. (2014). Poleward ocean heat transports, sea ice processes, and arctic sea ice variability in NorESM1-M simulations. *Journal of Geophysical Research: Oceans*, *119*, 2095–2108. https://doi.org/10.1002/2013JC009435

Sandø, A., Nilsen, J. E. O., Eldevik, T., & Bentsen, M. (2012). Mechanisms for variable North Atlantic-Nordic Seas exchanges. *Journal of Geophysical Research*, *117*, C12006. https://doi.org/10.1029/2012JC008177

Sein, D. V., Koldunov, N. V., Danilov, S., Wang, Q., Sidorenko, D., Fast, I., et al. (2017). Ocean modeling on a mesh with resolution following the local Rossby radius. *Journal of Advances in Modeling Earth Systems*, *9*, 2601–2614. https://doi.org/10.1002/2017MS001099

Skagseth, O. (2004). Monthly to annual variability of the Norwegian Atlantic slope current: Connection between the northern North Atlantic and the Norwegian Sea. *Deep Sea Research Part I: Oceanographic Research Papers*, *51*, 349–366.

Skagseth, O., Drinkwater, K. F., & Terrile, E. (2011). Wind- and buoyancy-induced transport of the Norwegian Coastal Current in the Barents Sea. *Journal of Geophysical Research*, *116*, C08007. https://doi.org/10.1029/2011JC006996

Skagseth, O., Furevik, T., Ingvaldsen, R., Mork, H., Orvik, K., & Ozhigi, V. (2008). Volume and heat transports to the Arctic Ocean via the Norwegian and Barents Seas. In R. R. Dickson, J. Meincke, & P. Rhines (Eds.), *Arctic-subarctic ocean fluxes: Defining the role of the Northern Seas in climate* (pp. 45–64). Dordrecht: Springer.

Skagseth, O., & Orvik, K. (2002). Identifying fluctuations in the Norwegian Atlantic Slope Current by means of empirical orthogonal functions. *Continental Shelf Research*, *22*, 547–563.

Smedsrud, L. H., Esau, I., Ingvaldsen, R. B., Eldevik, T., Haugan, P. M., Li, C., et al. (2013). The role of the Barents Sea in the Arctic climate system. *Reviews of Geophysics*, *51*, 415–449. https://doi.org/10.1002/rog.20017

Spielhagen, R., Werner, K., Sorensen, S., Zamelczyk, K., Kandiano, E., Budeus, G., et al. (2011). Enhanced modern heat transfer to the Arctic by warm Atlantic Water. *Science*, *331*, 450–453.

Steele, M., Morley, R., & Ermold, W. (2001). PHC: A global ocean hydrography with a high quality Arctic Ocean. *Journal of Climate*, *14*, 2079–2087.

Wang, Q., Danilov, S., Jung, T., Kaleschke, L., & Wernecke, A. (2016). Sea ice leads in the Arctic Ocean: Model assessment, interannual variability and trends. *Geophysical Research Letters*, *43*, 7019–7027. https://doi.org/10.1002/2016GL068696

Wang, Q., Danilov, S., & Schröter, J. (2008). Finite element ocean circulation model based on triangular prismatic elements, with application in studying the effect of vertical discretization. *Journal of Geophysical Research*, *113*, C05015. https://doi.org/10.1029/2007JC004482

Wang, Q., Danilov, S., Sidorenko, D., Timmermann, R., Wekerle, C., Wang, X., et al. (2014). The Finite Element Sea Ice-Ocean Model (FESOM) v.1.4: Formulation of an ocean general circulation model. *Geoscientific Model Development*, *7*, 663–693.

Wang, Q., Ilicak, M., Gerdes, R., Drange, H., Aksenov, Y., Bailey, D. A., et al.(2016a). An assessment of the Arctic Ocean in a suite of interannual CORE-II simulations. Part II: Liquid freshwater. *Ocean Modelling*, *99*, 86–109.

Wang, Q., Ilicak, M., Gerdes, R., Drange, H., Aksenov, Y., Bailey, D. A., et al. (2016b). An assessment of the Arctic Ocean in a suite of interannual CORE-II simulations. Part I: Sea ice and solid freshwater. *Ocean Modelling*, *99*, 110–132.

Wang, Q., Wekerle, C., Danilov, S., Koldunov, N., Sidorenko, D., Sein, D., et al. (2018). Arctic sea ice decline significantly contributed to the unprecedented liquid freshwater accumulation in the Beaufort Gyre of the Arctic Ocean. *Geophysical Research Letters*, *45*, 4956–4964. https://doi.org/10.1029/2018GL077901

Wang, Q., Wekerle, C., Danilov, S., Wang, X., & Jung, T. (2018). A 4.5 km resolution Arctic Ocean simulation with the global multi-resolution model FESOM 1.4. *Geoscientific Model Development*, *11*, 1229–1255.

Wekerle, C., Wang, Q., Danilov, S., Schourup-Kristensen, V., von Appen, W.-J., & Jung, T. (2017). Atlantic Water in the Nordic Seas: Locally eddy-permitting ocean simulation in a global setup. *Journal of Geophysical Research: Oceans*, *122*, 914–940. https://doi.org/10.1002/2016JC012121

Wekerle, C., Wang, Q., von Appen, W.-J., Danilov, S., Schourup-Kristensen, V., & Jung, T. (2017). Eddy-resolving simulation of the Atlantic Water circulation in the Fram Strait with focus on the seasonal cycle. *Journal of Geophysical Research: Oceans*, *122*, 8385–8405. https://doi.org/10.1002/2017JC012974

Yeager, S., Karspeck, A., & Danabasoglu, G. (2015). Predicted slowdown in the rate of Atlantic sea ice loss. *Geophysical Research Letters*, *42*, 10,704–10,713. https://doi.org/10.1002/2015GL065364

Zhang, J., Rothrock, D., & Steele, M. (1998). Warming of the Arctic Ocean by a strengthened Atlantic Inflow: Model results. *Geophysical Research Letters*, *25*, 1745–1748.